Structural basis for engineering of retinoic acid receptor isotype-selective agonists and antagonists

Martine Géhin, Valérie Vivat, Jean-Marie Wurtz, Régine Losson, Pierre Chambon, Dino Moras and Hinrich Gronemeyer

Background: Many synthetic retinoids have been generated that exhibit a distinct pattern of agonist/antagonist activities with the three retinoic acid receptors (RARα, RARβ and RARγ). Because these retinoids are selective tools with which to dissect the pleiotropic functions of the natural pan-agonist, retinoic acid, and might constitute new therapeutic drugs, we have determined the structural basis of their receptor specificity and compared their activities in animal and yeast cells.

Results: There are only three divergent amino acid residues in the ligand binding pockets (LBPs) of RARα, RARβ and RARγ. We demonstrate here that the ability of monospecific (class I) retinoid agonists and antagonists to bind to and induce or inhibit transactivation by a given isotype is directly linked to the nature of these residues. The agonist/antagonist potential of class II retinoids, which bind to all three RARs but depending on the RAR isotype have the potential to act as agonists or antagonists, was also largely determined by the three divergent LBP residues. These mutational studies were complemented by modelling, on the basis of the three-dimensional structures of the RAR ligand-binding domains, and a comparison of the retinoid agonist/antagonist activities in animal and yeast cells.

Conclusions: Our results reveal the rational basis of RAR isotype selectivity, explain the existence of class I and II retinoids, and provide a structural concept of ligand-mediated antagonism. Interestingly, the agonist/antagonist characteristics of retinoids are not conserved in yeast cells, suggesting that yeast co-regulators interact with RARs in a different way than the animal cell homologues do.

Address: Institut de Génétique et de Biologie Moléculaire et Cellulaire (IGBMC), CNRS/INSERM/ULP/Collège de France, BP 163, 67404 Illkirch Cedex, C.U. de Strasbourg, France.

Correspondence: Hinrich Gronemeyer
E-mail: hg@igbmc.u-strasbg.fr

Key words: retinoids, retinoic acid receptors, selectivity

Received: **19 March 1999**
Revisions requested: **16 April 1999**
Revisions received: **5 May 1999**
Accepted: **6 May 1999**

Published: **9 July 1999**

Chemistry & Biology August 1999, **6**:519–529
http://biomednet.com/elecref/1074552100600519

 ISSN 1074-5521

Introduction

Three retinoic acid receptors (RARα, RARβ and RARγ) and three retinoid X receptors (RXRα, RXRβ and RXRγ), members of the nuclear receptor (NR) superfamily [1], mediate the biological effects of retinoic acids (all-*trans* and 9-*cis* retinoic acids; t-RA and 9c-RA) upon development, cell differentiation and proliferation, and homeostasis [1–5]. RARs, which bind t-RA or 9c-RA, and RXRs, which bind only 9c-RA, form heterodimers and act as ligand-dependent transcriptional regulators. Crystal structure data [6–8] and a structure-based alignment [9] of the NR ligand-binding domains (LBDs) have led to a general model of NR function: binding of either agonist or antagonist induces a major structural transition of the carboxy-terminal part of the LBD comprising helix H11, loop 11–12 and helix H12. This positions helix H12, which comprises the conserved core of the activation function-2 (AF-2 AD), the presence and integrity of which is essential for agonist-induced transactivation [1,2], in a new LBD environment. Note that additional changes occur, for example, at the levels of helix H3 and the Ω-loop, which together result in a compaction of the LBD. It is believed that the repositioning of helix H11 upon ligand binding initiates the LBD transconformation. Upon agonist binding, helix H12 in its new environment contributes to the generation of a surface to which LXXLL (using single-letter amino acid code and where X denotes any amino acid) NR boxes of co-activators bind, as shown by both functional and co-crystallization studies ([10–12]; for reviews see [13,14]). Simultaneously the allosteric changes destabilize the interface between some NRs and co-repressors. The binding of (certain) antagonists also compacts the LBD in a similar way to that of agonists but steric constraints mean that helix H12 cannot bind in the agonist position and thus no co-activator-binding surface is generated. Instead, H12 binds to the groove that in agonist complexes is occupied by the LXXLL NR boxes of co-activators [12,13,15]. Note that the agonist-induced allosteric receptor transconformation is apparently also required for other ligand-dependent NR activities, such as the binding to target gene response elements *in vivo* [16,17] and the 'crosstalk' with other signal transduction

Figure 1

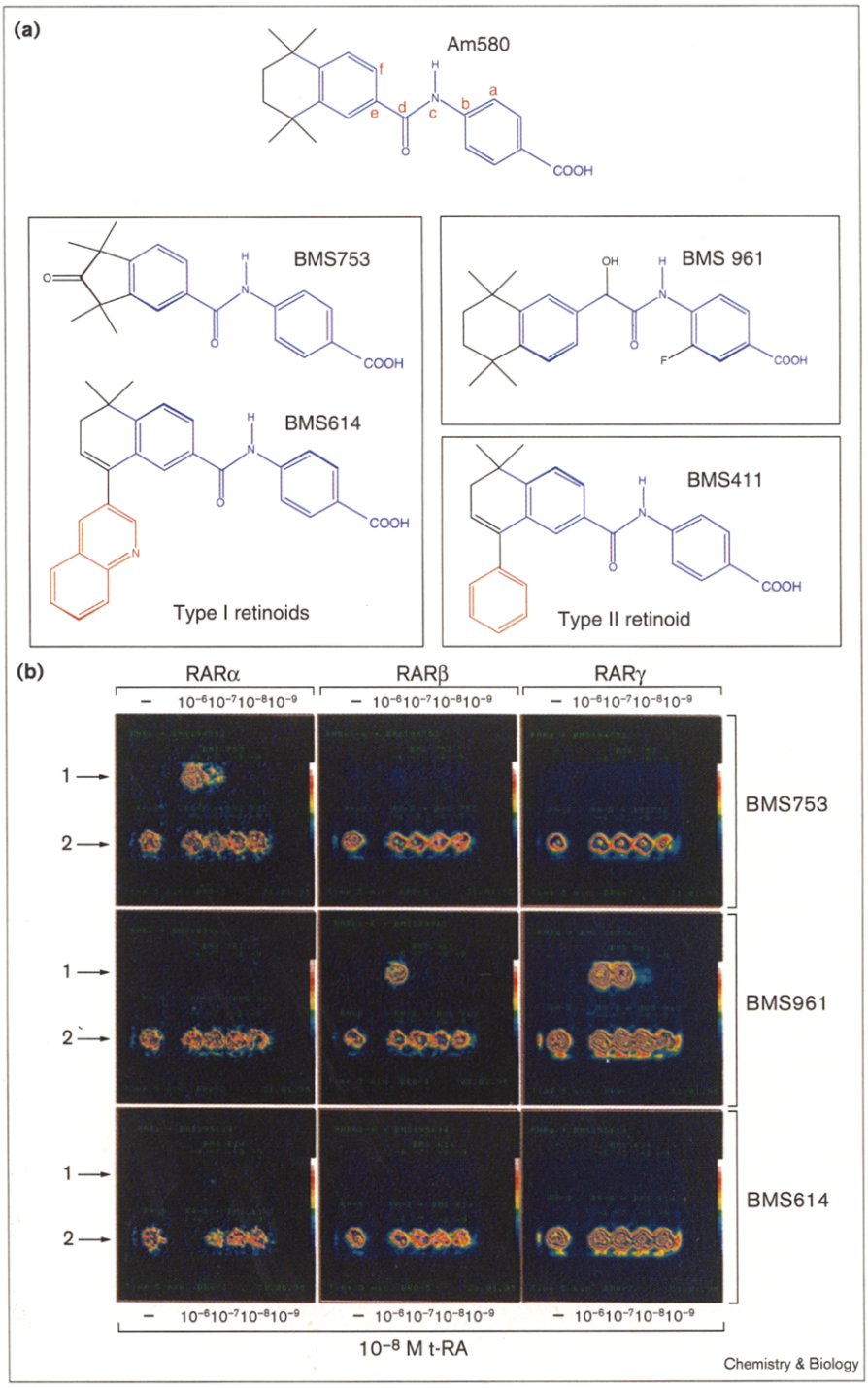

Chemical structures and agonistic/antagonistic activities of synthetic retinoids used in the present study. **(a)** Chemical structures of Am580, BMS753, BMS614, BMS961 and BMS411. Common structures are shown in blue, antagonistic substitutions in red; the dihedral angles discussed in the Materials and methods section on modelling are characterized by atoms a–f . **(b)** False colour representation of retinoid-induced luciferase activity in HeLa cells, stably transfected with the recombinant $(17\ m)_5$–G–luc and either GAL–RARα, GAL–RARβ, or GAL–RARγ, as indicated. As described previously [19], luciferase-induced bioluminescence was monitored *in vivo* using a single-photon-counting camera by seeding equal amounts of cells in a 24-well tissue culture plate and incubating them with increasing concentrations of BMS753, BMS961 or BMS614 alone ('1' lanes; revealing agonistic activities) or together with 10 nM all-*trans* retinoic acid ('2' lanes; revealing antagonistic activities), as indicated. Activities in the absence of ligand (– in the '1' lanes) and in the presence of 10 nM all-*trans* retinoic acid alone (– in '2' lanes) are shown for comparison. False colour representations were derived by using identical conditions for a given reporter cell line, except that the images of BMS753, BMS961 and BMS614 induction of the RARα reporter cells are shown at a higher sensitivity than for RARβ and RARγ reporter cells. Similar results have been obtained with several independently established reporter cell lines.

pathways, such as the mutual interference of the transactivation abilities of NRs and AP-1 (often referred to as transrepression; see [1,18]).

Synthetic retinoids can be described as acting in (at least) four ways: synthetic retinoids can act as agonists or antagonists, they can exhibit RAR or RXR selectivity, or they can show RARα, RARβ or RARγ isotype selectivity, and some retinoids can preferentially induce either target gene transactivation or AP-1 transrepression [19–21].

Here we demonstrate the existence of two distinct classes of retinoids in animal cells; class I retinoids interact with only one RAR isotype as either agonists or antagonists,

whereas class II retinoids exhibit similar affinities to, but distinct agonistic or antagonistic activities with, the RAR isotypes. We show that only the three divergent amino acid residues in the LBPs of RARα, RARβ and RARγ are responsible for the selective binding of class I monospecific synthetic retinoid agonists and antagonists. In addition, we provide evidence that these three residues are also specifically involved in determining the agonistic or antagonistic properties of class II retinoids. Furthermore, homology modelling based on the *holo*-RARγ three-dimensional structure suggests the structural basis that accounts for the isotype selectivity of the retinoids investigated in this study, as well as the probable mechanism of antagonism. Finally, we demonstrate that in yeast cells the agonist/antagonist pattern of synthetic retinoids diverges from that seen in animal cells, most probably because of the distinct sets of co-regulators expressed in the two types of cells.

Results and discussion

Two classes of synthetic retinoids

Studies of ligand binding and agonist/antagonist activities revealed the existence of at least two classes of synthetic retinoids: class I monospecific agonistic or antagonistic ligands like BMS753 and BMS614 (Figure 1a) that act specifically on a given RAR isotype (RARα in this case) even at the highest concentration tested (1 μM; Figure 1b) and either do not bind, or bind only very weakly, to the two other isotypes (Table 1, and data not shown); class II retinoids that bind, sometimes with very similar affinity (such as BMS411; Figure 1a and [19]) to all three RARs but act as agonists for a given RAR and as (partial) antagonists (relative to the natural ligand all-*trans* retinoic acid, t-RA) for another isotype [19].

To investigate the structural basis for the RAR isotype-specific agonistic/antagonistic activities of synthetic retinoids, we examined the role of the three divergent amino acid residues (see Table 2) that have been previously identified [7] in helices H3, H5 and H11 of the LBPs of RARα, RARβ and RARγ. Note that these differences refer only to the LBP; in the LBD there are a total of 51 amino acid changes between the three RARs. For each isotype these residues were mutated into the corresponding residues of the two other isotypes, and we analysed the effect of these mutations on ligand binding and transcriptional properties of the resulting LBP chimeric receptors in response to various synthetic retinoids.

The three divergent residues in the ligand-binding pockets of RARs are critically involved in the binding of class I monospecific retinoids

Mutation of the three divergent RARγ LBP residues into their RARα counterparts 'switched' the ligand specificity of the mutant RARγ(A234S, M272I, A397V); hereafter referred to as RARγ→α; Table 3) to that of RARα.

Table 1

Relative binding affinities for synthetic retinoids.

	K_i(nM)		
Receptor	BMS614	BMS753	BMS961
RARα	2.5	2.0	–
RARγ	–	–	1.5
RARγ→α	1.0	1.0	–

The RARγ→α mutant carries the three divergent LBP residues of the RARα in an RARγ background. The competition assays were performed with 5 nM tritiated t-RA, a range of synthetic ligand concentrations between 1 nM and 1 μM, and 500 nM nonradioactive t-RA to determine nonspecific binding. – Indicates that the corresponding synthetic ligand was not able to compete significantly with tritiated t-RA in the range of concentrations used.

RARγ→α responded as specifically as wild-type RARα did to the BMS753 agonist and the BMS614 antagonist (Figure 2a; lanes 7–9 and 13–15, respectively), whereas the response to the RARγ-selective agonist BMS961 was lost (Figure 2; lanes 10–12). A very similar switch in the ligand response repertoire was observed for the corresponding RARβ mutant when the only divergent residue between RARα and RARβ LBPs was mutated to the RARα identity (RARβA225S, termed RARβ→α; Figure 2b). Similarly, converting the LBP of RARα or RARβ into that of RARγ yielded mutants (RARα(S232A, I270M, V395A) termed RARα→γ and RARβ(V388A, I263M) termed RARβ→γ, respectively) displaying a RARγ-specific ligand response repertoire (Figures 2c,d). Finally, introducing the RARβ LBP-specific residues into either RARα (RARαS232A) or RARγ (RARγ(M272I, A397V)) resulted in mutants that had lost their RARα- or RARγ-specific ligand response characteristics (RARα→β and RARγ→β in Figures 2e,f). In this case only the loss of RARα or RARγ-specific responses could be determined, as no class I RARβ-monospecific retinoid is presently available. In summary, both the loss and the gain of function by the above mutants demonstrates that the response to class I monospecific retinoid

Table 2

Three divergent residues in the RAR ligand-binding pockets.

	Helices		
Receptor	H3	H5	H11
RARα	Ser232	Ile270	Val395
RARβ	Ala225	Ile263	Val388
RARγ	Ala234	Met272	Ala397

The three divergent residues in the LBPs of RARα, RARβ and RARγ, are located in helices H3, H5 and H11. The single residues differing between RARα and RARβ LBPs are displayed in red, those differing between RARβ and RARγ are shown in blue.

Table 3

Mutated LBDs with swapped LBP identity.

	Helices		
Receptor	H3	H5	H11
RARα→β	Ser→Ala	–	–
RARα→γ	Ser→Ala	Ile→Met	Val→Ala
RARβ→α	Ala→Ser	–	–
RARβ→γ	–	Ile→Met	Val→Ala
RARγ→α	Ala→Ser	Met→Ile	Ala→Val
RARγ→β	–	Met→Ile	Ala→Val

One, two and three mutations are necessary to change the RAR LBP identity from α→β, β→γ, and α→γ respectively.

agonists and antagonists is entirely dictated by the identity of, at most, the three RAR LBP-divergent residues. Since the present study was finished others [22] have reported a limited RAR LBD chimera analysis that is also in keeping with our original prediction [7] of a critical role for the divergent residues in retinoid selectivity. Importantly, the agonistic or antagonistic response of a given LBP chimeric receptor that had acquired new ligand specificity was identical to that of the wild-type receptor, which selectively binds this ligand.

To test whether or not the new ligand-specific response of the various chimeric mutants was correlated with a change in ligand-binding specificity, the ligand-binding characteristics of the *Escherichia coli*-expressed LBD of one mutant (RARγ→α; Table 3) was compared in *in vitro* competition experiments with those of the corresponding LBDs of RARα and RARγ. As expected, the RARγ→α LBD bound the RARα-specific retinoids BMS753 and BMS614 with

Figure 2

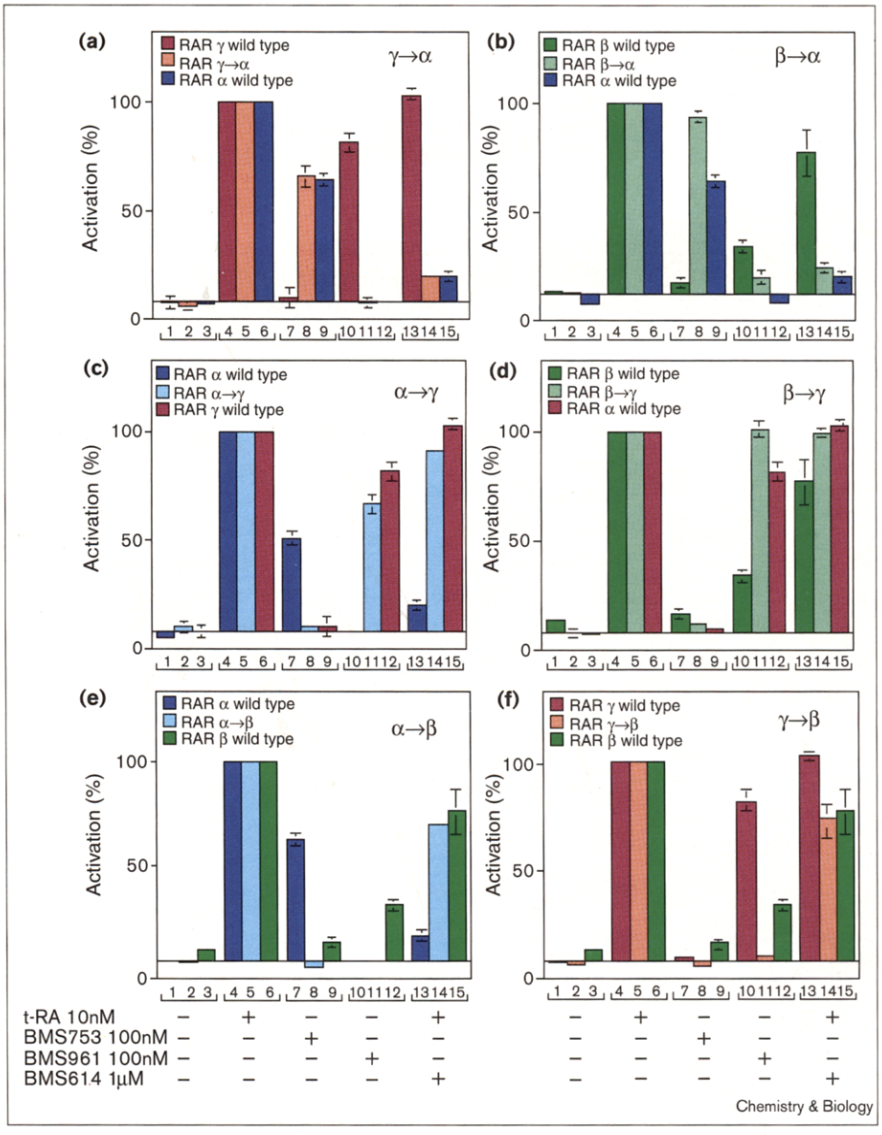

The three divergent residues in the LBP of RARα, RARβ and RARγ determine the RAR selectivity of monospecific (class I) retinoids. The results obtained with two retinoid agonists, the RARα-selective BMS753 and the RARγ and RARβ-selective BMS961, and one antagonist, the RARα-selective BMS614, are shown. Transient transactivation assays in the absence and presence of the various retinoids (indicated at the bottom of the figure) were performed with Cos cells and the TRE_3-tk-CAT reporter gene. Data are expressed relative to the maximal stimulation seen with t-RA (100%), which also corresponded to 0% antagonistic activity. The results obtained with the various mutants, together with the corresponding wild-type counterparts, are given in the following panels: **(a)** hRARγ→α (A234S, M272I, A397V); **(b)** hRARβ→α (A225S); **(c)** hRARα→γ (S232A, I270M, V395A); **(d)** hRARβ→γ (V388A, I263M); **(e)** hRARα→β (S232A); **(f)** hRARγ→β (M272I, A397V). RARα, blue; RARβ, green; RARγ, pink; mutants are depicted as bars with a paler colour of that of the parent receptor. Agonistic activities (lanes 4–12) are determined by exposing transfected cells to the retinoid alone, whereas antagonistic activities (lanes 13–15) are measured as the inhibition by a given retinoid of the transactivation seen in the presence of 10 nM t-RA. Note that BMS614 is devoid of any agonistic activity and that BMS753 and BMS961 do not display any antagonistic activity (see Figure 1b). The results shown correspond to the mean ± standard deviation (see error bars) of three transfections.

the same affinity as RARα, whereas no binding of the RARγ-selective retinoid BMS961 could be detected (Table 1). In conclusion, the functional specificity of the above monospecific synthetic retinoids is because of their RAR binding selectivity, which is itself determined by the identity of the residues that differ in the LBPs of RARα, RARβ and RARγ.

The three divergent RAR LBP residues also determine the RAR isotype-specific agonistic/antagonistic activity of class II retinoids

In contrast to class I retinoids, class II retinoids bind to all three RARs, sometimes with similar affinities [19], but the transcriptional outcomes of this interaction can be entirely different for each isotype. For example BMS411 and BMS453, typical class II retinoids, act as RARα and RARγ antagonists and RARβ agonists in stably transfected 'reporter' cells and *in vivo* [17,19]. These type II retinoids are, however, not completely devoid of agonist activity with RARα and RARγ, because they can induce some transcriptional activity in transient transfections when used alone, most probably because of high amounts of the expressed receptor and/or transfected reporter plasmid (Figure 3; [19]). Yet, this activity is weaker than that of t-RA or other class II agonists at similar concentrations, and is apparently insufficient to elicit a biological response *in vivo*, such as cell differentiation or target gene induction on its own [17,23,24].

To investigate the potential role of the three divergent LBP residues in the RAR isotype-specific response to the class II retinoid BMS411, we compared the agonistic (using 100 nM BMS411 alone) and antagonistic (reduction of 10 nM t-RA-induced activity by 1 μM BMS411) potentials for the three RAR isotypes and the chimeric RAR mutants in which LBPs were interconverted. Interestingly, when the LBP of RARγ was converted into that of RARβ, RARγ→β (Table 3) responded to BMS411 like RARβ did, that is BMS411 acted as a full agonist, whereas it was a mixed agonist/antagonist for the parental RARγ (Figure 3a). Similarly, BMS411 antagonised t-RA-induced activity of RARβ→α (Figure 3c) and RARβ→γ (Figure 3d) of which the LBPs were converted into those of RARα and RARγ, respectively. Also, by changing the

Figure 3

The divergent residues of the ligand-binding pocket are responsible for the agonistic/antagonistic activities of class II retinoids. Similar analysis as in Figure 2 to determine the agonist and antagonistic potential of BMS411 with wild-type (wt) and LBP mutant receptors, as indicated in each panel. Data are given relative to the maximal stimulation seen with t-RA (= 100%), which corresponds also to 0% antagonistic activity. The results obtained with the various mutants, together with the corresponding wild-type counterparts are given as follows: **(a)** hRARγ→β (M272I, A397V); **(b)** hRARα→β (S232A); **(c)** hRARβ→α (A225S); **(d)** hRARβ→γ (V388A, I263M). Data representation is as in Figure 2. Note that BMS411 is a RARβ agonist (see, for example, (a), lanes 9 and 12) and acts as RARα and RARγ antagonist relative to 10 nM t-RA ((a) and (b), compare lanes 4 and 10), but displays a weak agonist activity with RARα ((b), lane 7) and RARγ ((a), lane 7). The results shown correspond to the mean ± standard deviation (see error bars) of three transfections.

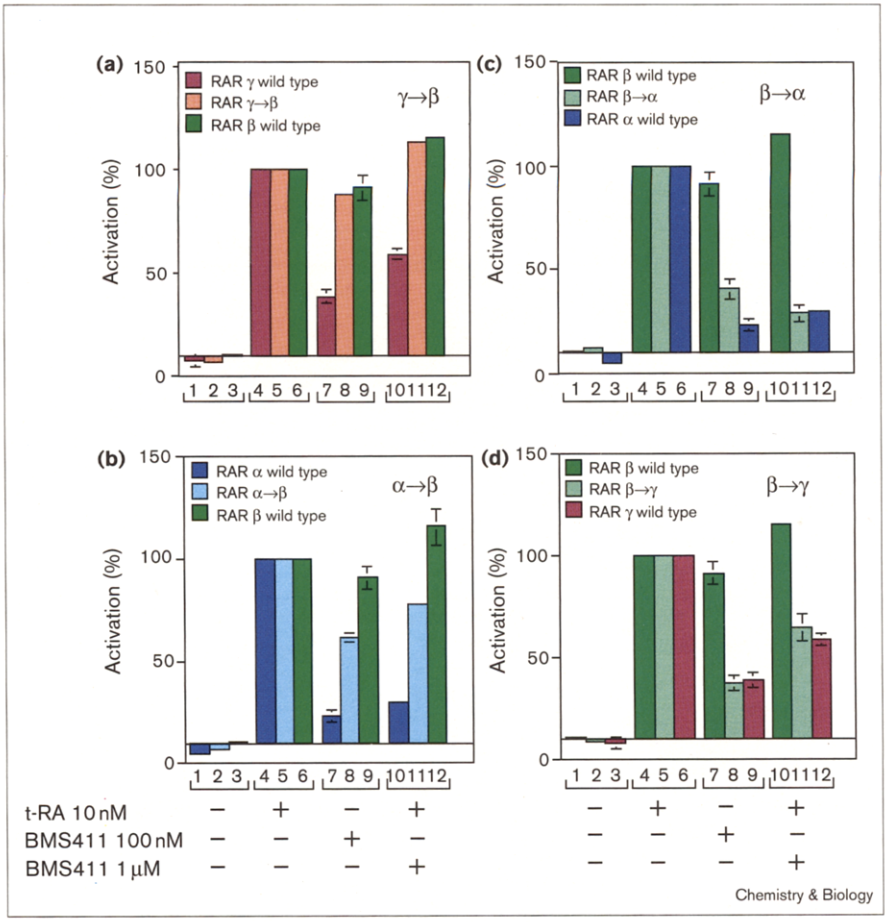

RARα LBP into that of RARβ, RARα→β acquired additional BMS411-induced agonistic potential when compared with RARα (Figure 3b). Thus, the three divergent residues in the RAR isotype LBPs not only determine the binding selectivity of class I retinoids but also the relative agonistic/antagonistic strength of class II retinoids.

Synthetic retinoids exert different agonistic/antagonistic potential in animal and yeast cells

The observation that BMS614 is a class I RARα antagonist under a variety of conditions (e.g. in different animal cells with different reporter gene promoters) could suggest that the BMS614–RARα complex possesses an intrinsic antagonistic potential. This is in contrast to class II retinoids, in which agonistic potential can significantly vary when different conditions are compared (data not shown). Surprisingly, however, BMS614 is a RARα agonist in yeast cells, inducing about 40% of the t-RA-induced transcriptional activity seen with RARα and the cognate reporter gene (Figure 4a). As expected from its isotype selectivity, BMS614 did not significantly affect RARβ or RARγ transactivation (Figures 4b,c). Also the agonistic/antagonistic potential of the type II retinoids BMS453 and BMS411 was entirely different in yeast and animal cells. Both ligands were classified as RARβ agonists of similar potency in the 'reporter' cell assay [19], BMS411 acted as a RARβ 'superagonist' in yeast cells, displaying nearly twice the agonistic potency of t-RA at 1 μM, but BMS453 was completely inactive (Figure 4b). With RARα and RARγ, BMS411 displayed significant agonistic activity in yeast, whereas BMS453 was moderately active with RARα and nearly inactive with RARγ (Figures 4a,c).

The co-regulators mediating RAR-dependent transactivation in yeast are unknown and could not be used to investigate the mechanistic basis of BMS614 agonistic activity. But the observation that a co-repressor binding-disabled RARα mutant displayed a weak agonistic response with BMS614 [25] could suggest that the antagonistic activity of BMS614 might be related to the presence of co-repressors in animal cells [26,27] and the absence of such factors could possibly account for its agonistic potential in yeast cells. Co-expressing the silencing mediator for retinoid and thyroid hormone receptors (SMRT) [27] did not reduce the RARα agonistic activity of BMS614 in yeast cells (data not shown), suggesting that if SMRT can form a functional co-repressor complex in yeast, its absence does not explain the BMS614 agonist activity.

Together, the above results indicate that although nuclear receptors can transactivate in yeast cells, the involved co-regulator complexes interact very differently with the receptor than their animal cell counterparts. This is most probably caused by the interaction of the yeast cell co-regulators with receptor surfaces that are different from those interacting with animal cell co-regulators. Apparently, synthetic retinoids can induce receptor conformations that differentiate between these interfaces. These results indicate that the agonist/antagonist potential of class II retinoids might also vary in animal cells expressing distinct sets of co-

Figure 4

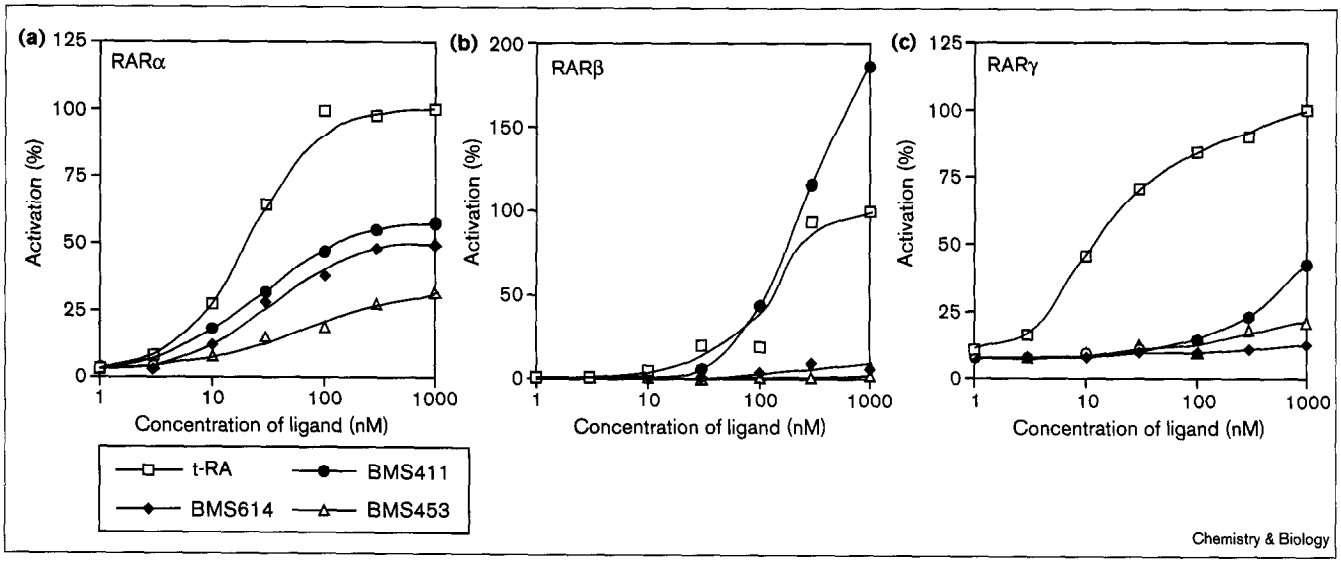

Synthetic retinoids have different agonistic/antagonistic characteristics in yeast. Transcriptional activities in response to BMS614 (RARα-selective antagonist in mammalian cells), BMS411 and BMS453 were assayed in stably transformed yeast lines, established with ERE3X-URA3 reporter gene and **(a)** RARα–ER-CAS, **(b)** $RAR\beta_2$–ER-CAS, and **(c)** RARγ(DEF)–ER-CAS. Receptor activities were revealed by OMPdecase assays. Data are expressed relative to the maximal stimulation seen with 1 μM t-RA (= 100%). The values obtained fall into the range of the mean ± 20% of three assays.

regulators. Obviously, such a scenario provides the conceptual basis for cell-selective retinoid agonists and antagonists.

Structural basis of RAR isotype selectivity towards the class I retinoid BMS753

To understand the role of the three divergent RAR LBP residues in determining ligand-binding selectivity, we modelled these pockets according to the three-dimensional structure of *holo* RARγ LBD [7]. Figures 5a and 6a (monoviews and stereoviews, respectively) show the RARα LBP into which BMS753 has been docked (see the Materials and methods section for details). The structural basis of its RARα selectivity is readily deduced from this model. A hydrogen bond can be established between the amino group of the retinoid and RARαS232, whereas in both RARβ and RARγ this hydrogen bond is lost. The replacement of Ser232 with an alanine residue (Table 2), most likely accounts for the much lower relative affinity of BMS753 to RARβ and RARγ and for the acquisition of binding affinity by the mutant RARγ→α (Table 1, and data not shown).

Proposed mechanism for the antagonistic action of BMS614, an RARα-selective ligand

Our generally accepted concept [7,9] that the agonist-induced transconformation of the LBD, involving most notably H12 (which encompasses the core of the ligand-dependent AF-2 activation domain), generates the surfaces for co-activator interaction predicts that ligands inducing an alternate positioning of H12 should act as antagonists of the AF-2 function of nuclear receptors. This hypothesis has recently been confirmed by crystallisation of the oestrogen receptor complexes with oestradiol or the AF-2 antagonist raloxifen or tamoxifen [12,15].

The RARα antagonist BMS614 can be viewed as a quinolyl derivative of the RARα agonist Am580 [28] (Figure 1a). Modelling of BMS614 in the RAR LBPs without major adaptations of the sidechains was possible only when H12 was removed. For RARα two conformers of BMS614, termed conformers I and II, could be docked into the ligand-binding cavity. The amino group of conformer I (white in Figure 5c; blue in Figure 6c) is used for hydrogen bonding to Ser232, whereas the keto group of conformer II (green in Figure 6c) is oriented towards Ser232, albeit with a bad hydrogen bond geometry. No H-bond can be established in RARβ, which has an alanine residue at the position corresponding to Ser232 (Table 2), thus accounting for the very weak relative binding affinity (~20–50-fold lower than for RARα; Table 1 and data not shown). In addition to lacking the hydrogen bond, the RARγ model predicts steric interference with Met272 which 'pushes' the ligand into a position where steric clashes occur not only with H12 residues of the *holo*-LBD but also with the Cβ of Ala397 in H11 (data not shown). Together these RARγ features probably account for an RARγ binding affinity of BMS614 that is too low to be determined in classical competition assays (Table 1).

Indeed, attempts to add back helix H12 in the three-dimensional model of the H12-less RARα LBP–BMS614 complex revealed that the quinolyl group precludes a proper positioning of H12 in its active conformation because of steric clashes with Ile410 (Figure 6c), thus most probably accounting for the RARα antagonistic nature of BMS614. This hypothesis is further strengthened by modelling of the LBD of the so-called RARα 'AHT' (Ala–His–Thr) triple mutant [26]. We have observed that this mutation converts the antagonistic response of RARα to BMS614 to a (weak) agonistic one, both in heterodimers with RXRα [25], as well as in GAL-RARα chimeras (about 8% of the transactivation seen with Am80 on the same 17mer-tk-CAT reporter gene; data not shown). Originally

Figure 5

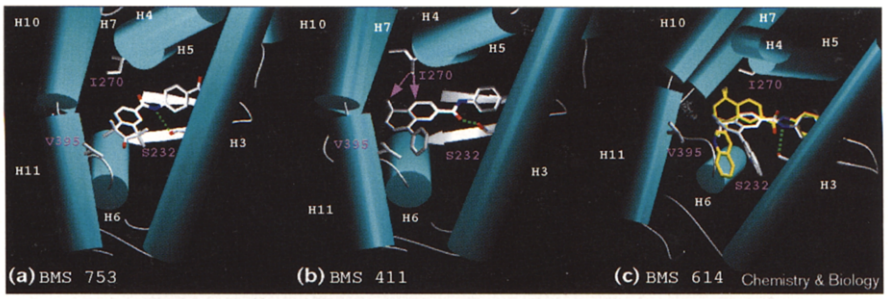

Models of BMS753, BMS411 and BMS614 in the LBP of RARα. **(a)** The RARα-selective agonist BMS753 can be docked into the RARα LBP in the presence of H12 (removed for illustration purposes) in its *holo* position; the hydrogen bond established between the ligand amino group and RARαSer232 is illustrated as a green dotted line. **(b)** BMS411 in a complex with the H12-less RARα LBP (conformer II, white ligand). BMS411 can bind in the alternate conformation I (not shown), which has the amide linker oriented as BMS753 in Figure 5a. Steric contacts with RARαIle270 that do not exist in the case of BMS753 are illustrated as arrows. **(c)** The RARα-selective type I antagonist BMS614 in the LBP of RARα BMS614 can bind as two distinct conformers: conformer I (white) establishes the hydrogen bond to RARαSer232 via the amine like BMS753 in (a), whereas conformer II (not shown; analogous to conformer II of BMS411 in Figure 5b) uses its carboxyl group for hydrogen bonding to the same serine residue. Ligand docking was done without helix H12 (white ligand) or without helix H1 (yellow ligand, see text). The three RARα-specific residues in the LBP that diverge in RARβ and RARγ are indicated in purple (see Table 2 for the divergent LBP residues), nitrogen is shown in blue, oxygen in red. The figure was prepared with the program SETOR.

Figure 6

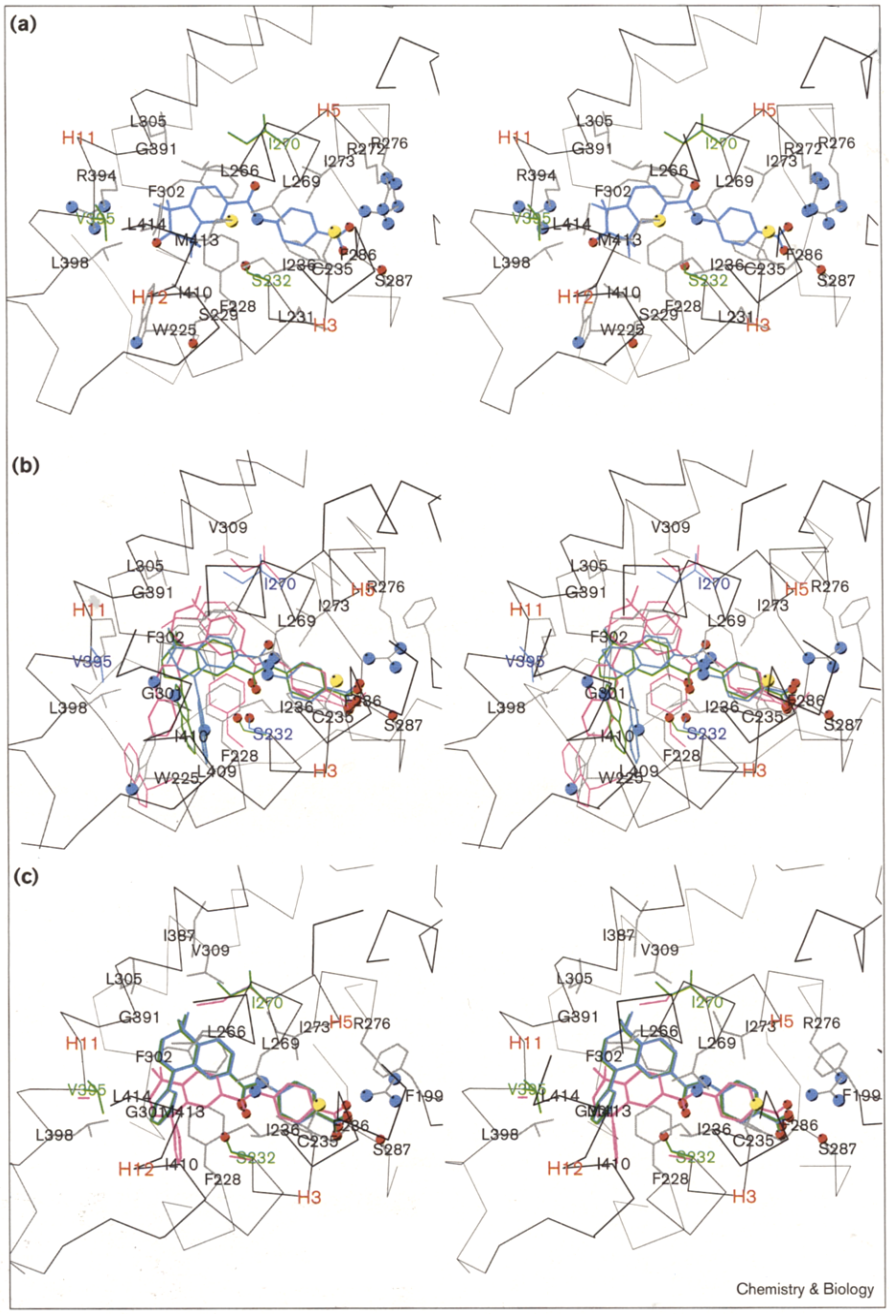

The selectivity of RAR isotype binding and agonist/antagonist potential of synthetic retinoids can be revealed by modelling. **(a)** Stereoview of the RARα-selective type I agonist BMS753 (blue) in the LBP of RARα modelled according to the crystal structure of *holo*-RARγ [7,29]. Ligand docking was done in presence of H1 and H12. The residues and positions shown are those of RARα; the three RARα-specific residues that diverge in RARβ and RARγ are shown in green; oxygens in red, nitrogens in blue and sulphur as yellow spheres; some helices are shown in red to facilitate orientation. **(b)** Stereoview of conformer II (see text) of BMS411 in the LBP of RARα (blue ligand), RARβ (green ligand) and RARγ (pink ligand). C_α tracing (helices H3, H5, H11 and H12 are indicated) with the sidechains of the three divergent residues (Table 2) in the ligand color code; several invariant sidechains are shown in grey. Ligand docking was done without helix H12, which was subsequently added to reveal possible steric interference between the ligand and H12 residues. Positioning of H12 was possible for RARα and RARβ, but required major sidechain adaptations for RARγ. **(c)** Stereoview of the RARα-selective type I antagonist BMS614 in the LBP of RARα. Ligand docking was done without H12 and subsequent H12 addition (green and blue ligands) or without H1 in presence of H12 (pink ligand). Note that in the first case BMS614 can bind as two distinct conformers: conformer I (blue) establishes the hydrogen bond to RARα Ser232 via the amine like BMS753 in (a), whereas conformer II (green; analogous to conformer II of BMS411 in Figure 5b) uses its keto group for hydrogen bonding to the same serine residue. Note the steric interference for both conformers between the quinolyl group and the H12 residue RARα Ile410, indicating that both conformers of BMS614 exert antagonistic activity. Only conformer II docks into the H1-less LBP of RARα when H12 is in the *holo* position (pink ligand). Note that the carboxylate anchoring network [7] is slightly rotated around the long arm of the L-shaped ligand allowing the quinolyl moiety of the ligand to penetrate deeper into the ligand cavity provided some residue sidechains adapt (displayed in pink). The three RARα-specific residues that diverge in RARβ and RARγ are shown in green and blue according to the color code of the two conformers; note the different positions of the RARα Ser232.

this mutant was used as a co-repressor binding-disabled receptor [26] and we pointed out that these residues are involved in tethering helix H1 to the core of the LBD [13]; the triple mutation disrupts this interaction and should liberate H1, thereby leading to co-repressor dissociation. Modelling of the RARα LBP without H1 is a good approximation to mimic (at least some of) the structural consequences of mutating the AHT residues. Interestingly, in contrast to the wild-type LBD, the BMS614 conformer II can be docked into the H1-less RARα LBP with the anchoring carboxylate moiety slightly shifted (yellow and pink ligands in Figures 5c and 6c, respectively) relative to its position in the H12-less LBD (green ligand in Figure 6c) and might therefore account for the agonistic effect of BMS614 on the AHT-mutant. The rotation along the long arm of the L-shaped ligand allows the bulky

quinolyl group to penetrate deeper into the cavity, thus reducing the steric interference with H12 residues. Full penetration requires some adaptation of LBP residue sidechains (purple in Figure 6c); this restriction might be responsible for the weakness of the agonistic activity of BMS614 with this mutant.

Agonist/antagonist properties of the type II retinoid BMS411

BMS411 is similar to BMS614 and can also be viewed as a derivative of Am580, but the quinolyl group of BMS411 is replaced by a less bulky phenyl group in BMS614 (Figure 1a). Relative to t-RA, BMS411 acts as an RARα antagonist with some agonistic potential, and as an RARβ agonist. As for Am580 [28], our previous ligand binding data [19] demonstrated that the relative binding affinity of BMS411 for RARα was approximately 10-fold and 100-fold higher than for RARβ and RARγ, respectively. BMS411 can adopt two conformations in the RARα LBP orientating either the amino (conformer I; similar orientation of the linker group as in BMS753 in Figure 5a) or the keto (conformer II; Figure 5b; blue ligand in Figure 6b) moiety towards Ser232. In contrast to conformer I, conformer II can only establish a suboptimal hydrogen bond, as its keto group sterically interferes with the serine residue thus forcing the ligand to move towards Ile270 residue in H5. Importantly, only the position of the less favoured conformer II is compatible with the *holo* position of H12 and is expected to exert some agonistic activity. Conformer I generates significant steric interference with Ile410 of *holo* H12 that could account for the antagonistic potential of BMS411 with RARα.

The differential possibility of BMS411 to establish a hydrogen bond in the LBP of RARβ is likely to account for the lower affinity of RARβ than RARα [19]. The RARβ agonistic activity of this retinoid is possibly the consequence of its ability to adopt both an antagonistic and an agonistic conformation in the binding pocket. In contrast to RARα (see above), the antagonistic conformer I cannot be stabilised by hydrogen bonding in the LBP of RARβ, thus favouring the binding of conformer II (green in Figure 6b), which does not interfere with H12 *holo* positioning. Accordingly, BMS411 generates a weak agonistic RARβ activity [19].

Modelling of BMS411 in the LBP of RARγ required major adaptations of sidechains. Such adaptations are, however, unlikely to occur when considering our previous observation that three RARγ ligands, all-*trans* and 9-*cis* retinoic acid and the synthetic RARγ-specific ligand BMS961, adopt a very similar three-dimensional structure in the RARγ LBP, indicating a rigid pocket into which the ligand has to fit [29]. In the absence of H12, BMS411 can be accommodated without major sidechain adaptations in the RARγ LBP. The ligand occupies a position that is very different from that in the RARα and RARβ LBPs (pink ligand in Figure 6b). This is because of residue Met272 (which in RARγ replaces the isoleucine residue of RARα and RARβ; see Table 2) that sterically interferes with the dimethyl group and pushes the ligand away. Addition of H12 to the model reveals, however, that in this position a steric clash occurs between the ligand phenyl group and Ile412 in H12 (Figure 6c). In addition, the amide carboxyl group of BMS411 gets close to Ala234, causing additional steric hindrance. Together with the inability of establishing a stabilising hydrogen bond as in RARα, these steric interferences most probably account for the 100-fold lower binding affinity of BMS411 for RARγ relative to RARα (no attempt was made to structurally interpret the very weak RARγ agonist activity of BMS411 that can only be seen in transient transfection experiments).

Significance

All-*trans* retinoic acid (t-RA) exerts highly pleiotypic activities during embryonic development and in the adult by regulating cell growth, death and differentiation. These activities are mediated by three retinoid receptors (RARα, RARβ and RARγ) and three rexinoid receptors (RXRα, RXRβ and RXRγ). Despite its chemotherapeutic and chemopreventive potential [30], the pharmacological use of the natural ligand is severely restricted because of its diverse activities. The synthesis of ligands that induce only a subset of nuclear receptor (NR) activities and/or interact only with some receptor isotypes might overcome these restrictions [19,31,32]. To this end, our results provide new insights into the molecular aspects of an NR–ligand interaction leading to isotype-selective agonistic and antagonistic transcriptional effects that can be understood from a combination of functional and structural analyses. These principles provide for the first time structural guidelines for the design of ligands with predetermined characteristics. Because of the apparent conservation of their overall structure, the NR superfamily should be an excellent model system for rational drug design. Notably, our results show that the agonist/antagonist activities of synthetic retinoids differ between yeast and animal cells. This suggests that ligands with cell-type-specific activities can be found, possibly related to a divergent expression (pattern) of coregulators.

Materials and methods

Recombinants

To generate the mutations a double PCR strategy was used. Briefly, the hRARα sequence from nucleotide 370 to the 3′ end of the coding sequence, the entire coding sequence of hRARβ and the hRARγ sequence from nucleotide 343 to the stop codon were PCR-amplified using pSG5-based RARα, RARβ and RARγ vectors, respectively, as templates, Deep Vent Polymerase (Biolabs), and the appropriate oligonucleotides. The sequences of these primers are available on request. The mutated PCR fragments were digested by *Sac*I and *Xma*I for hRARα, *Xho*I and *BamH*I for hRAR β, *Sac*I and *BamH*I for hRARγ and inserted into the corresponding sites of the pSG5-based wild-type

RARα, RARβ and RARγ expression vectors. The yeast chimeric receptors were expressed from the multicopy expression plasmid YEp90, which contains an expression cassette under the control of PGK promoter. RARα1–ER-CAS, in which the native DNA binding domain (DBD; region C) of RARα1 was replaced with the DBD cassette of the human ERα(ER-CAS; residues 185–250) and the cognate ERE3X-URA3 reporter gene have been described previously [33]. RARγ(DEF)–ER-CAS has been constructed from the RARα–ER-CAS, in which the DEF region of RARα was replaced by the DEF region of human RARγ (residues 156–454). RARβ2–ER-C contains the complete DBD of the human ERα receptor (ER-C; residues 176–282) separated by two amino acids glycine and threonine from the A/B region of human RARβ2 (residues 1–80) on the amino-terminal side and by three amino acids Ala–Arg–Glu from the DEF region (residues 147–448) of the human RARβ2 on the carboxy-terminal side. Details concerning each construction are available upon request.

Transactivation assays

Cos 1 and HeLa cells were plated in Dulbecco's modified Eagle's medium (DMEM, Gibco) supplemented with 5% charcoal-treated foetal calf serum (FCS) at a density of 1.5×10^6 cells per dish, and transfected as described [34] with 200 ng of the respective RAR mutant expression vector, 200 ng of the RXRα expression vector, 2 μg of the reporter gene (TRE3 tk CAT or DR5 tk CAT [35–37]), 500 ng of CMV-βGAL as an internal control to account for variations of transfection efficiency, and 7 μg pBluescript as a carrier. After transfection (24 h), cells were treated for 16 h with various concentrations of ligands before washing with 1 × phosphate buffered saline (PBS). The cells were collected in 1 ml TEN (10 mM Tris-HCl, pH 7.5; 1 mM EDTA; 150 mM NaCl) and pelleted for 2 min at 13,000 rpm at 4°C. Cell pellets were resuspended in 200 μl lysis buffer (250 mM Tris-HCl, pH 7.5; 15% glycerol; 5 mM DTT), disrupted by three cycles of freezing and thawing and centrifuged for 5 min at 13,000 rpm at 4°C. CAT was quantified by enzyme-linked immunosorbent assay (ELISA) (Boehringer Mannheim). Yeast transactivation assays were performed as described [38].

Expression of mutants

BL21 bacteria were transformed with pET15b-based vectors that express the mutated LBDs of RARs. Bacteria were grown overnight in LB supplemented with 100 μg/ml ampicillin. These precultures (15 ml) were grown in 500 ml LB to an optical densities at 600nm between 0.45 and 0.5 and IPTG was added to a final concentration of 1 mM. After 2.5 h, cells were pelleted and resuspended in 6.5 ml ice-cold binding buffer (5 mM imidazol; 0.5 M NaCl; 20 mM Tris-HCl, pH 8). Bacteria were lysed with 100 μg/ml lysozyme during 30 min on ice and then for 5 min at 37°C. The lysate was sonicated in ice for 1 min, diluted with 1 volume of ice-cold binding buffer and re-sonicated for 1 min. The homogenate was centrifuged for 30 min at 30,000 rpm. The bacterial extract was then adjusted to 10% glycerol and stored at −80°C.

Ligand-binding assays

Synthetic retinoids, resuspended in ethanol, were mixed with tritiated all-*trans* retinoic acid (t-RA; 5 nM) with or without 100-fold excess of non-radioactive t-RA (500 nM). Ethanol was evaporated in the dark. A sample of the bacterial extracts (200 μl) were added to these tubes in which the synthetic ligand concentration varied from 0.1 nM to 1 μM. The mixture was incubated for 4 h at 4°C in the dark. Each assay was performed in duplicate. 150 μl of the extract were put onto glassfiber filters (Whatman GF/C) and filtered under vacuum. The filters were washed with 30 ml of buffer (10 mM Tris-HCl, pH 8; 150 mM NaCl; 0.01% Triton X100) and the remaining radioactivity was assayed by scintillation counting. IC_{50} and K_i values were determined from the corresponding competition curves [39].

Receptor modelling and ligand docking

The models of the human RAR isotypes are based on the recently solved crystal structures of the *holo*-hRARγ LBD in complexes with RAs or a synthetic ligand [7,20]. The RAR isotypes differ in the binding niche hRARγ to obtain the pseudo hRARα (A234S, M272I and A397V) and pseudo hRARβ (M272I and A397V). Models of truncated receptors missing either helix H1 (residues 215–419 in hRARγ) or helix H12 (residues 182–406 in hRARγ) of all three isotypes were also constructed. The Quanta/Charmm (Molecular Simulations Inc.) and O [40] packages were used throughout the work. Before docking the ligands BMS753, BMS614 and BMS411 in the binding niche of the different receptors we performed a conformational search analysis to identify the low energy conformers of BMS753. With the grid scan algorithm of the Quanta/Charmm package the two rotatable bonds of BMS753 (around the dihedral angles 'abcd' and 'defg' in Table 1a) were changed by steps of 15° from 0 to 360° and the energy for each conformer calculated. The energy was obtained by restraining the dihedrals and energy minimising the ligand with the Powell procedure for 200 steps. The contour map revealed that the 'defg' dihedral angle can range from 150 to 210° (less than 1 kcal/mol from the global minimum) bringing the CO group of the linker away from the bulky substituent of BMS614 or BMS411 and either below or above the aromatic cycle. The 'abcd' dihedral angle adopts preferentially four values: +40° ± 20°, +150° ± 20°, −150° ± 20° and −40° ± 20°. The conformers I and II discussed in the text are located close to the −150° and 40° minima. The cavity volume of the binding niche of the entire receptor isotypes have been calculated in the program O with Voidoo [41] and used as a guide during the docking process. One of the cavities calculated by Voidoo gives the volume accessible to the center of the probe-sphere (1.4 Å radius) that is in contact with the protein's van der Waals surface. In this representation of the cavity most of the apolar heavy atoms should lie inside the calculated volume. The three ligands were then fitted manually taking the two liganded hRARγ crystal structures, the cavity volumes and the preferred conformations as landmarks. From this analysis only two conformers can be fitted in the LBP were the 'abcd' dihedral adopts either the −150° ± 20° or +40° ± 20° values. The all-atom force field as generated by Quanta/Charmm, has been used for the protein and the ligands. The C_α backbone atoms of the receptors have been fixed during energy minimisations. The complexes were energy-minimised for 2000 steps with a dielectric constant of 4 using the Powell procedure.

Acknowledgements

Bristol-Myers Squibb kindly provided the synthetic retinoids used in this study. We are grateful to Ghislaine Christoffel for the characterization of synthetic retinoids with the reporter cell system, Thierry Lerouge for providing the RARα, RARβ, RARγ(D_3E)/pET15b expression vectors, and Margarita Cervino for yeast OMPdecase assays; we thank Jean-Marie Garnier, Astrid Pornon and Cathie Erb for technical advice, and the services for cell culture, DNA sequencing, oligonucleotides synthesis, and computer-assisted design for support. This work was supported by funds from the INSERM, CNRS, HUS, Fondation pour la Recherche Médicale, the Ministère de la Recherche et de la Technologie, le Collège de France, the EC BIOMED Progamme (BMH4-CT96-0181 to HG and DM), and Bristol-Myers Squibb.

References

1. Gronemeyer, H. & Laudet, V. (1995). Nuclear receptors. *Protein Profile* **2**, 1173-1308.
2. Chambon, P. (1996). A decade of molecular biology of retinoic acid receptors. *FASEB J.* **10**, 940-954.
3. Mangelsdorf, D.J., *et al.*, & Evans, R.M. (1995). The nuclear receptor superfamily: the second decade. *Cell* **83**, 835-839.
4. Mangelsdorf, D.J. & Evans, R.M. (1995). The RXR heterodimers and orphan receptors. *Cell* **83**, 841-850.
5. Kastner, P., Mark, M. & Chambon, P. (1995). Nonsteroid nuclear receptors: what are genetic studies telling us about their role in real life? *Cell* **83**, 859-869.
6. Bourguet, W., Ruff, M., Chambon, P., Gronemeyer, H. & Moras, D. (1995). Crystal structure of the ligand-binding domain of the human nuclear receptor RXR-α. *Nature* **375**, 377-382.
7. Renaud, J.P., Rochel, N., Ruff, M., Vivat, V., Chambon, P., Gronemeyer, H. & Moras, D. (1995). Crystal structure of the RAR-γ ligand-binding domain bound to all-*trans* retinoic acid. *Nature* **378**, 681-689.
8. Wagner, R.L., Apriletti, J.W., McGrath, M.E., West, B.L., Baxter, J.D. &

9. Wurtz, J.M., *et al.*, & Gronemeyer, H. (1996). A canonical structure for the ligand-binding domain of nuclear receptors. *Nat. Struct. Biol.* **3**, 87-94.
10. Darimont, B.D. *et al.*, & Yamamoto, K.R. (1998). Structure and specificity of nuclear receptor-coactivator interactions. *Genes Dev.* **12**, 3343-3356.
11. Nolte, R.T. *et al.*, & Milburn, M.V. (1998). Ligand binding and co-activator assembly of the peroxisome proliferator-activated receptor-gamma. *Nature* **395**, 137-143.
12. Shiau, A.K. *et al.*, & Greene, G.L. (1998). The structural basis of estrogen receptor/coactivator recognition and the antagonism of this interaction by tamoxifen. *Cell* **95**, 927-937.
13. Moras, D., & Gronemeyer, H. (1998). The nuclear receptor ligand-binding domain: structure and function. *Curr. Opin. Cell. Biol.* **10**, 384-391.
14. Torchia, J., Glass, C., & Rosenfeld, M.G. (1998) Co-activators and co-repressors in the integration of transcriptional responses. *Curr. Opin. Cell. Biol.* **10**, 373-383.
15. Brzozowski, A.M., *et al.*, & Carlquist, M. (1997). Molecular basis of agonism and antagonism in the oestrogen receptor. *Nature* **389**, 753-758.
16. Dey, A., S. Minucci & K. Ozato. (1994). Ligand-dependent occupancy of the retinoic acid receptor beta 2 promoter *in vivo*. *Mol. Cell Biol.* **14**, 8191-8201.
17. Chen, J.Y., *et al.*, & Gronemeyer, H. (1996). Two distinct actions of retinoid-receptor ligands. *Nature* **382**, 819-822.
18. Resche-Rigon, M. & Gronemeyer, H. (1998). Therapeutic potential of selective modulators of nuclear receptor action. *Curr. Opin. Chem. Biol.* **2**, 501-507.
19. Chen, J.Y. *et al.*, & Gronemeyer, H. (1995). RAR-specific agonist/antagonist which dissociate transactivation and AP1 transrepression inhibit anchorage-independent cell proliferation. *EMBO J.* **14**, 1187-1197.
20. Fanjul, A., *et al.*, & Pfahl, M. (1994). A new class of retinoids with selective inhibition of AP1 inhibits proliferation. *Nature* **372**, 107-111.
21. Nagpal, S., Athanikar, J. & Chandraratna, R.A. (1995). Separation of transactivation and AP1 antagonism functions of retinoic acid receptor alpha. *J. Biol. Chem.* **270**, 923-927.
22. Ostrowski, J., Roalsvig, T., Hammer, L., Starret, J. Jr., KuLong, J. & Reczek, P. (1998). Serine 232 and methionine 272 define the ligand binding pocket in retinoic acid receptor subtypes. *J. Biol. Chem.* **273**, 3490-3495.
23. Roy, B., Taneja, R. & Chambon, P. (1996). Synergistic activation of retinoic acid (RA)-responsive genes and induction of embryonal carcinoma cell differentiation by an RA receptor alpha (RAR alpha)-, RAR beta- or RAR gamma-selective ligand in combination with a retinoid X receptor-specific ligand. *Mol. Cell. Biol.* **15**, 6481-6487.
24. Taneja, R., *et al.*, & Chambon, P. (1996). Cell-type and promotor-context dependent retinoic acid receptor (RAR) redundancies for RAR beta 2 and Hoxa-1 activation in F9 and P19 cells can be artefactually generated by gene knockouts. *Proc. Natl Acad. Sci. USA* **93**, 6197-6202.
25. Vivat, V., *et al.*, & Chambon, P. (1997). A mutation mimics the ligand-induced transconformation of the retinoid X receptor. *EMBO J.* **16**, 5697-5709.
26. Hörlein, A.J., *et al.*, & Rosenfeld, M.G. (1995). Ligand-independent repression by the thyroid hormone receptor mediated by a nuclear receptor co-repressor. *Nature* **377**, 397-403.
27. Chen, J.D. & Evans, R.M. (1995). A transcriptional co-repressor that interacts with nuclear hormone receptors. *Nature* **377**, 454-457.
28. Kagechika, H., Kawachi, E., Hashimoto, Y., & Shudo, K. (1986). Differentiation inducers of human promyelocytic leukemia cells HL60. Phenylcarbamoylbenzoic acid and polyene amides. *Chem. Pharm. Bull.* **34**, 2275-2278.
29. Klaholz, B.P., *et al.*, & Moras, D. (1998). Conformational adaptation of ligands to the human nuclear receptor RARγ. *Nat. Struct. Biol.* **5**, 199-202.
30. Hong, W.K. & Sporn, M.B. (1997) Recent advances in chemoprevention of cancer. *Science* **278**, 1073-1077.
31. Ekena, K., Katzenellenbogen, J.A., & Katzenellenbogen, B.S. Determinants of ligand specificity of estrogen receptor-alpha: estrogen versus androgen discrimination. (1998). *J. Biol. Chem.* **273**, 693-699.
32. Peet, D.J., Doyle, D.F., Corey, D.R., & Mangelsdorf, D.J. (1997). Engineering novel specificities for ligand-activated transcription in the nuclear hormone receptor RXR. *Chem. Biol.* **5**, 13-21.
33. Heery, D.M., Zacharewski, T., Pierrat, B., Gronemeyer, H., Chambon, P., & Losson, R. (1993). Efficient transactivation by retinoic acid receptors in yeast requires retinoid X receptors. *Proc. Natl Acad. Sci. USA* **90**, 4281-4285.
34. Bocquel, M.T., Kumar, V., Stricker, C., Chambon, P. & Gronemeyer, H. (1989). The contribution of the N- and C-terminal regions of steroid receptors to activation of transcription is both receptor- and cell-specific. *Nucleic Acids Res.* **17**, 2581-2595.
35. Nagpal, S., Saunders, M., Kastner, P., Durand, B., Nakshatri, H. & Chambon, P. (1992). Promoter context- and response element-dependent specificity of the transcriptional activation and modulating functions of retinoic acid receptors. *Cell* **70**, 1007-1019.
36. Mader, S., Chen, JY., Chen, Z., White, J., Chambon, P.,& Gronemeyer, H. (1993). The patterns of binding of RAR, RXR and TR homo- and heterodimers to direct repeats are dictated by the binding specificities of the DNA binding domains. *EMBO J.* **12**, 5029-5041.
37. Mader, S.,Leroy, P., Chen, JY., & Chambon, P. (1993). Multiple parameters control the selectivity of nuclear receptors for their response elements. *J. Biol. Chem.* **268**, 591-600.
38. vom Baur, E., *et al.*, & Losson, R.(1996). Differential ligand-dependent interactions between the AF-2 activating domain of nuclear receptors and the putative transcriptional intermediary factors mSUG1 and TIF1. *EMBO J.* **15**, 110-124.
39. Chen, Y. & Presof W.H. (1973). Relationship between the inhibition constant (Ki) and the concentration of inhibitor which causes 50% inhibition (IC50) of an enzymatic reaction. *Biochem. Pharmacol.* **22**, 3099-3108.
40. Jones, T. A., Zou, J. Y., Cowan, S. W. & Kjeldgaard, M. (1991). Improved methods for binding protein models in electron density maps and the location of errors in these models. *Acta Crystallogr. A* **47**, 110-119.
41. Kleywegt, GJ & Jones, TA. (1994). Detection, delineation, measurement and display of cavities in macromolecular structures. *Acta Crystallogr. D* **50**, 178-185.

Because *Chemistry & Biology* operates a 'Continuous Publication System' for Research Papers, this paper has been published via the internet before being printed. The paper can be accessed from http://biomednet.com/cbiology/cmb – for further information, see the explanation on the contents pages.